Published in final edited form as:
Environ Sci Technol. 2010 December 1; 44(23): 9030–9035. doi:10.1021/es102129d.

Label-Free Chemiresistive Immunosensors for Viruses

Dhammanand J. Shirale[1], **Mangesh A. Bangar**[1], **Miso Park**[1], **Marylynn V. Yates**[2], **Wilfred Chen**[1], **Nosang V. Myung**[1], and **Ashok Mulchandani**[1]

[1]Department of Chemical and Environmental Engineering, Riverside, CA 92521, USA

[2]Department of Environmental Sciences, University of California, Riverside, CA 92521, USA

Abstract

We report development, characterization and testing of chemiresistive immunosensors based on single polypyrrole (Ppy) nanowire for highly sensitive, specific, label free, and direct detection of viruses. Bacteriophages T7 and MS2 were used as safe models for viruses for demonstration. Ppy nanowires were electrochemically polymerized into alumina template and single nanowire based devices were assembled on a pair of gold electrodes by ac dielectrophoretic alignment and anchored using maskless electrodeposition. Anti-T7 or anti-MS2 antibodies were immobilized on single Ppy nanowire using EDC-NHS chemistry to fabricate nano-biosensor for the detection of corresponding bacteriophage. The biosensors showed excellent sensitivity with a lower detection limit of 10^{-3} plaque forming unit (PFU) in 10 mM phosphate buffer, wide dynamic range and excellent selectivity. The immunosensors were successfully applied for the detection of phages in spiked untreated lake water samples. The results show the potential of these sensors in health care, environmental monitoring, food safety and homeland security for sensitive, specific, rapid and affordable detection of bioagents/pathogens.

Keywords

Bacteriophage; virus; nanowire; immunosensor; label-free; polypyrrole

Introduction

Detection of viruses is central to human health care, environmental monitoring and even bioterrorism prevention [1, 2]. Rotavirus is one of the examples that occur through shellfish grown in polluted water and contaminated drinking water [3–5]. Rotavirus is a genus of double-stranded RNA virus in the family Reoviridae. It is the leading single cause of severe diarrhoea among infants and young children [6]. By the age of five, nearly every child in the world has been infected with rotavirus at least once [7]. Poliovirus infections can be subclinical or can cause mild illness, aseptic meningitis, or poliomyelitis. Coxsackievirus infection is the most common cause of viral heart disease [8, 9]. Thus detection of these infectious and potentially deadly pathogens is of paramount importance from a human health point of view.

Conventional methods of virus detection range from cell culture to immunological to molecular techniques [10–13]. Cell culture-based methods, which remain as the gold standard as it is the only method that detects infective virus particles, while able to detect a single infective particle per sample, is extremely slow taking up to several weeks to produce results [14]. Amplification of viral nucleic acid using the polymerase chain reaction (PCR)

Correspondence to: Ashok Mulchandani.

or reverse transcription-PCR (RT-PCR for the detection of mRNA) is extensively used as a research tool for the analysis of environmental samples [15]. PCR-based methods provide the benefit of rapid analysis at relatively low cost, but they are extremely sensitive to contaminants, which become highly concentrated during sample processing, which can lead to false-negative results.

Immunological methods such as radioimmunoassay, immunofluorescence or enzyme-linked immunosorbent assay (ELISA) are widely used in the medical diagnostics and gaining acceptance in environmental monitoring [16]. However, use of labels, and lack of sensitivity, specificity, speed, and portability limit the use of these techniques for field applications. These limitations highlight the need for economic analysis technique/device that can perform simple, label-free, rapid and potentially point-of-care/field-deployable detection of viruses with high specificity and sensitivity.

Recently, one-dimensional nanostructures, such as nanowires, nanotubes, and nanofibers, have been attracting considerable attention in electronic circuits, chemical and electrochemical sensors, photovoltaic cells, electrochromic devices, and biosensors applications due to their unique geometry with low dimension, large surface-to-volume ratio and their versatility for electrical and optical detection [17–26]. Nanostructures such as silicon nanowires and carbon nanotubes have been applied for label-free chemiresistive/field effect transistor (FET) based biosensor applications for rapid and sensitive detection of various important analytes including viruses [27–31]. However, nanostructures made out of conducting polymers hold great promise due to their economic and easy electrochemical/chemical synthesis, easy chemical modifications, excellent electrical properties and most importantly, bio-compatibility. Conducting polymer are semiconductors with excellent electrical properties in terms of their conductivity range and easy modulation using either the gate potential or composition. They exhibit excellent electrical properties as a semiconductor channel for semiconductor devices such as transistors, sensors and electromechanical devices [32–34]. Specifically, single conducting polymer nanowire based devices are increasingly gaining importance in the field of biomedical science as a single nanowire based device geometry allows precise control on the sensor characteristics while eliminating the indeterminate nanowire to nanowire contact in a nano-network based sensor [35]. Thus in this study, we have fabricated template directed polypyrrole (Ppy) nanowires for single nanowire based device assembly. EDC-NHS chemistry [35] was used for surface functionalization of Ppy nanowire with either polyclonal anti-T7 or monoclonal anti-MS2phage antibodies. Functionalized chemiresistive Ppy nanowire devices were then used for the detection of different T7 and MS2 bacteriophage concentrations in the range of 1×10^{-3} PFU to 1×10^{9} PFU in 10 mM, pH 7.0 phosphate buffer (PB). In order to show its potential application for samples without pretreatment, we have demonstrated detection of T7 and MS2 phages in untreated lake water samples (collected from Davis near Folsom, CA). In this work MS2 and T7 bacteriophages were used as safe representative species for viruses (a diameter of 25 nm and 55 nm, respectively). T7 phage is especially simple to grow and replicates faster than MS2, a filamentous phage; plaques are formed within 3 hours at 37°C and cultures are lysed within 1–2 hours after infection. Besides, the T7 phage particle is extremely robust, and is stable to harsh conditions that inactivate other phages [36]. Above and beyond being safe for laboratory work, MS2 phage has been used as an indicator in previous researches because it has similar size, shape and type of nucleic acid (RNA) of waterborne viral pathogens such as enteroviruses, caliciviruses, and rotaviruses [37,38]. Moreover, they are more suitable to be used in scenarios where use of actual viruses is hampered by the possibility of introducing potential pathogens into drinking water treatment plants, shellfish-growing waters, or foodstuffs [39].

METHODS

Bacteriophages Preparation

The T7 phages were prepared and quantified as described in reference [40]. The overnight culture of BLT 5403 strain of *E. coli* was incubated in TB (terrific broth) medium including 100 μg/ml of ampicillin with shaking for 3–4 hours at 37°C (OD_{600} = 0.6–0.8), and then a phage stock was infected to amplify lysates on logarithmically growing cells. Lysis was observed after incubating with shaking at 37°C for 1–2 hours. Phage sample was collected by centrifugation at 8,000 × g for 10 min. The titer was phages per milliliter, was determined by plaque assays. *E. coli* HS(pFamp)R host strain was also incubated and infected with MS2 phage [12] in medium containing 1% tryptone, 0.05% glucose, 0.8% NaCl, 0.03% $CaCl_2$, and 15μg/ml each of ampicillin and streptomycin. Overnight amplified MS2 phages were collected and quantified in the same way as T7 phage.

Polypyrrole Nanowires Synthesis

Ppy nanowires were electrochemically synthesized using well established template directed electrodeposition technique [41,42]. Alumina membrane of 200 nm pore size and 60 μm thickness (Whatman International Ltd, Maidstone, England) was used as a scaffold for nanowire fabrication. Seed layer was deposited by sputtering ~200 nm thick gold using the Emitech K550 (Emitech Ltd., Kent, England) sputter coater on one side of the alumina template. Electrodeposition was carried out in a three electrode cell with the gold-coated alumina template as working electrode, Ag/AgCl as reference and platinum coated titanium strip as counter electrode using a CH Instrument Model 760C (CH Instruments, Austin, TX, USA) electrochemical analyzer. 0.5 M pyrrole (Sigma Aldrich) in 0.2 M $LiClO_4$ (Aldrich, Milwaukee WI USA) was used as an electrolyte solution. Chronocoulometry method was used for electrodepositing Ppy nanowires by passing 0.7 C charge at 0.9 V. The gold seed layer was removed using 0.15 M KI in 0.1 N I_2 gold-etchant solution. After washing the alumina template with water, it was dissolved in 30% H_3PO_4 acid (Acros organic) and briefly sonicated to free the nanowires to form a suspension. Nanowires were washed with nanopure water and resuspended in nanopure water. The suspension was diluted 10-fold for further use.

Single Nanowire Device Fabrication

Chromium (Cr) adhesion layer of 200 A° and 1800 A° thick gold (Au) contact layer were deposited on (100) oriented Silicon wafer with 300 nm SiO_2 layer. An array of 16 pairs of gold microelectrodes with ~70 μm separation between adjacent pairs with each pair containing rectangular electrodes of ~55 μm width separated by 3 μm gap were used as contact electrodes for device assembly as shown in Figure 1 (a). These electrodes were cleaned with piranha solution (3.5 ml of concentrated H_2SO_4 + 1.5 ml of H_2O_2) (Fisher Scientific, Fair Lawn, New Jersey, USA). The two sides of 16-pairs were shorted to form two terminals. Ppy nanowires were aligned in the electrode gap by passing alternating current field of 4 MHz frequency and 3 V peak to peak between the two terminals. A 2 μl drop of Ppy nanowire suspension was dispensed on it and alignment was carried out for about a minute. To achieve single nanowire connection between a pair of contact electrodes as in Figure 1 (b), excess nanowires were physically/manually removed using a probe tip made out of 25 μm diameter gold wire under a 1000× magnification optical microscope. In order to secure the Ppy nanowire on to the gold electrodes, the nanowire was anchored with maskless electrodeposition (Figure 1 (c)), using chronoamperometry method (CH Instrument Model 760C Electrochemical Analyzer). A three-electrodes electrochemical cell consisting of the 16-pairs of contact electrodes with single Ppy nanowire connections as the working electrode, Ag/AgCl as a reference electrode and a platinum coated metal strip as a counter electrode was used. The electrolyte was Technigold (Technic Inc., California, USA)

at pH of 7.0 and the deposition potential used was −0.5 V vs Ag/AgCl at room temperature for 10 min for built up of ~300 nm thick gold layer on the gold electrode surface.

Polypyrrole Nanowire Biological Functionalization

Single Ppy nanowire devices were incubated for 3 hrs in 10 μl of 60 mM 1-Ethyl-3-[3-dimethylaminopropyl]carbodiimide hydrochloride (EDC) (Sigma Chemical Co. St Louis MO USA) solution in 0.1 M MES buffer at a resulting pH of <5.5, mixed with 100 μl N-hydrosuccinimide (NHS) in dimethyl sulfoxide (DMSO) (2 mg/mL) (Thermo Fisher Scientific, Rockford, IL, USA) and 10 μl anti-T7 (Millipore Corporate Billerica, MA, USA) or anti-MS2 antibody (Tetracore, Inc. Rockville, MD USA) as shown in Figure 1 (d). The excess reagent was subsequently removed and the devices were washed with 1% Tween-20 in PB buffer (PBT) followed by PB. To block nonspecific interactions between biomolecules and the nanowire, devices were incubated in BSA (1 mg/mL) (Sigma-Aldrich Inc., Missouri, USA) solution in PB (Figure 1 (e)). The excess BSA was removed, and the devices were washed with PBT followed by PB.

Sensing Measurements

Sensors were characterized in terms of their current-voltage (I–V) (Figure 2 and 3) response, measured using a semiconductor parameter analyzer (model 4155A, Agilent Technologies Inc., California) with a 10 μL drop of PB on the nanowire (wet condition). The voltage was swept from −200 to +200 mV, and the current was recorded. The nanowire resistance was measured as the inverse of the slope of I–V curve near zero voltage in the linear range of ±100 mV. I–V curves were measured before and after the sensor was incubated in respective analyte solution for 5 min followed by washing with PBT and finally with PB. Change in the sensor resistance was observed upon exposure to different concentrations of bacteriophages spiked in either 10 mM PB or untreated lake water samples.

AFM Imaging

A 0.5 ml suspension of the template grown Ppy nanowires was functionalized with anti-T7 antibody using the EDC-NHS chemistry followed by blocking with BSA as described above, washed three times with PBST and resuspended in PBST. A 2 μl of this nanowires suspension was dispensed on two mica surfaces for AFM imaging, in one case directly and the other after incubation with 1×10^9 PFU T7 phage for 5 min and washing with PB. AFM imaging was performed in tapping mode using Veeco Inova SPM.

RESULTS AND DISCUSSION

Single Ppy nanowire-based nanobiosensor was fabricated according to the technique developed in our laboratory [36] and characterized in terms of their resistance, surface morphology and sensing response. Because the maskeless gold electrodeposition anchoring was performed under conditions (pH 7 and −0.5 V vs. Ag/AgCl for 10 min) that can potentially de-dope Ppy and thus render the wire insulating, nanowire conductivity was determined before and after anchoring. An insignificant change in the nanowire conductivity after anchoring in comparison to before the maskless electrodeposition (data not shown) indicated there was no adverse effect of conditions used for gold electrodeposition on Ppy conductivity. Furthermore, the final device conductivity (10^0–10^1 S/cm) was in the reported range of conductivity for bulk and nanostructured Ppy, confirming conducting state of the polymer [43–49].

A single Ppy nanowire based sensor works on the principle of gating effect wherein, the semiconducting nanowire connected between the two contact electrodes is extremely sensitive to its surface environment and shows changes in its electrical properties to even

slight perturbations on its surface such as changes in ions/pH or adsorption of charged molecules on the surface. The binding of the negatively charged moieties such as antibodies and phage particles on the Ppy, a well-known p-type semiconductor [50], nanowire surface decreases the number of charge carriers (holes), thus increasing the nanowire resistance [51–53]. Figures 2A and 2B (trace (a)) show the I–V curves for bare Ppy nanowires. Functionalization of the Ppy nanowire with anti-T7 (Figure 2A, trace (b)) and anti-MS2 (Figure 2B, trace (b)) (and blocking step) increased the device resistance. This increase could arise due to chemical gating effect from the presence of negatively charged antibodies (and BSA) on p-type semiconducting Ppy nanowire surface [51] The increase of nanowire resistance upon antibody immobilization (and blocking) indicated successful functionalization (and blocking). Subsequent incubation of these anti-T7 and anti-MS2 functionalized nanowire with the corresponding target bacteriophage particles produced a dramatic increase in resistance (Figure 2A (c) and 2B (c)), illustrating the conductometric sensing.

As a further/additional proof to the presence of the antibody on the nanowire and the interaction/binding of the target antigen, AFM studies were done on a bare Ppy nanowire and an anti-T7 functionalized Ppy nanowire before and after antigen binding. Figure 3 (a) shows the AFM image and the height profile of a bare Ppy nanowire. The surface roughness of a bare Ppy nanowire measured using a line profile along the nanowire axis was around 1.5 nm ± 0.5 nm. After functionalization the surface roughness increased to 4 nm ± 1 nm (Figure 3 (b)) and was around 55 – 60 nm (Figure 3 (c)) when T7 phage interacted with anti-T7 functionalized Ppy nanowire. These changes in the surface roughness of the Ppy nanowire are indicative of the presence of antibody on the nanowire surface and subsequent phage binding to the antibody on the nanowire surface, confirming the successful antibody immobilization strategy as well as high affinity between antibody and its complementary target phage.

Figures 4 and 5 show the anti-T7 and anti-MS2 functionalized Ppy nanowire sensor responses [$(R - R_0)/R_0$, where R is the resistance after exposure to T7 or MS2 phage and R_0 is the initial sensor resistance], respectively, as a function of logarithmic T7 or MS2 phage concentration in 10 mM PB. As shown, anti-T7 and anti-MS2 functionalized Ppy nanowire sensors were extremely sensitive with a response of 0.74 ± 0.05 and 1.96 ± 0.9 even at the lowest tested concentration of 10^{-3} PFU, respectively. Further, sensors had a wide dynamic range spanning from 10^{-3} to 10^6 PFU. A 10^{-3} value of detected PFU can be attributed to the probability that all the phage particles in the stock culture are not infective and are hence not accounted by the infectivity assay technique used for standardizing the phage stock and/or that there can be up to 10^3 viral particles/PFU [54, 55]. Also, the MS2 phage sensor showed almost 3-fold greater response compared to that of T7 phage sensor at the saturation, which could be attributed to the extent of individual antibody immobilization which controls the binding capacity of the sensor or the difference in the surface charge density of the two phages or both. The limit of detection (LOD) for our single Ppy nanowire immunosensor is comparable to that reported for single silicon nanowire-based immunosensor for influenza type A virus and paramyxovirus [29,30] and two to three orders of magnitude better than that obtained for label-free immunosensing using quartz crystal microbalance, surface plasmon resonance and opto-fluidic ring resonator transducers [56–58].

Specificity is a critical issue for successful application of a sensor. A very low response of 0.18 ± 0.03 for 10^8 PFU of T7 phage was recorded on nanowire sensor functionalized with monoclonal anti-MS2 antibody. On the other hand, nanowire functionalized with polyclonal anti-T7 showed a response of 0.55 ± 0.3 when exposed to 10^8 PFU MS2. This cross-reactivity was, however, very small compared to the affinity between the antibodies and the respective target phages. Negative controls, nanowires without antibodies but blocked with

BSA, showed a response of only 0.02 ± 0.07 even for very high (10^8) PFU of both phages. The above results confirm the high selectivity of both phage immunosensors. However, there could be other phages or viruses that could cross-react and need to be identified with further experimentation.

The utility of the developed sensor for detection of T7 and MS2 in untreated field samples was further evaluated by measuring different T7 and MS2 concentrations spiked in untreated lake water samples (Figures 4 and 5). As shown, the lower detection limit, dynamic range, and sensitivity of the biosensor for T7 and MS2 in lake water sample was quantitatively comparable to that in PB. This indicates that the sensors are highly specific towards their respective target and also showed no response towards the other constituents present in the field water sample. Once again, these observations are limited for only the water sample tested and other water samples could present potential interferents.

In conclusion, we have successfully developed a highly sensitive and selective single Ppy nanowire chemiresistive sensor device for the rapid and label-free detection of bacteriophage. The methodology developed in this study can be readily extended for fabrication of nano-biosensor for detection of other viruses, proteins, etc. by using an appropriate recognition molecule. Small size, easy and fast electrical transduction mechanism, and the ability to integrate modern day electronics are the anticipated advantages of these sensors for detection at the point of care/use. As demonstrated, these sensors can be used for untreated sample analysis without the need for extensive sample preparation. As reported earlier [35], due to the array architecture of these devices and due to limited cross-reactivity of these sensors towards non-complementary targets, multi-analyte sensing/multi-plexing using an array of sensors functionalized with different functional recognition molecules is within reach.

Acknowledgments

We acknowledge the support of grants GR-83237501 from the U.S. EPA and CBET-0617240 from NSF and U01ES016026 from NIH.

References

1. Bolashikov ZD, Melikov AK. Methods for Air Cleaning and Protection of Building Occupants from Airborne Pathogens. Building and Environment. 2009; 44:1378–1385.
2. Baram M. Biotechnological Research on the Most Dangerous Pathogens: Challenges for Risk Governance and Safety Management. Safety Science. 2009; 47:890–898.
3. Gratacap-Cavallier B, Genoulaz O, Brengel-Pesce K, Soule H, Innicenti-Francillard P, Bost M, Gofti L, Zmirou D, Seigneurin JM. Detection of Human and Animal Rotavirus Sequences in Drinking Water. Appl. Environ. Microbiol. 2000; 66:2690–2692. [PubMed: 10831460]
4. Le Guyader F, Haugarreau L, Miossec L, Dubois E, Pommepuy M. Three-Year Study To Assess Human Enteric Viruses in Shellfish. Appl. Environ. Microbiol. 2000; 66:3241–3248. [PubMed: 10919776]
5. Verheyen J, Timmen-Wego M, Laudien M, Boussaad I, Sen S, Koc A, Uesbeck A, Mazou F, Pfister H. Detection of Adenoviruses and Rotaviruses in Drinking Water Sources Used In Rural Areas of Benin, West Africa. Appl. Environ. Microbiol. 2009; 75:2798–2801. [PubMed: 19270143]
6. Teran CG, Teran-Escalera CN, Villarroel P. Nitazoxanide vs. Probiotics for the Treatment of Acute Rotavirus Diarrhea in Children: A Randomized, Single-Blind, Controlled Trial in Bolivian Children. International Journal of Infectious Diseases. 2009; 13:518–523. [PubMed: 19070525]
7. Parashar UD, Hummelman EG, Bresee JS, Miller MA, Glass RI. Global Illness and Deaths Caused by Rotavirus Disease in Children. Emerging Infectious Diseases. 2003; 9:565–572. [PubMed: 12737740]

8. McWilliam Leitch EC, Harvala H, Robertson I, Ubillos I, Templeton K, Simmonds P. Direct Identification of Human Enterovirus Serotypes in Cerebrospinal Fluid by Amplification and Sequencing of the VP1 Region. Journal of Clinical Virology. 2009; 44:119–124. [PubMed: 19135410]
9. Sepúlveda RT, Zhang J, Watson RR. Selenium Supplementation Decreases Coxsackievirus Heart Disease during Murine AIDS. Cardiovascular Toxicology. 2002; 2:53–61. [PubMed: 12189280]
10. González-Techera A, Vanrell L, Last JA, Hammock BD, González- Sapienza G. Phage Anti-Immune Complex Assay: General Strategy for Noncompetitive Immunodetection of Small Molecules. Anal. Chem. 2007; 79:7799–7806. [PubMed: 17845007]
11. El-Sagheer AH, Brown T. Synthesis and Polymerase Chain Reaction Amplification of DNA Strands Containing an Unnatural Triazole Linkage. J. Am. Chem. Soc. 2009; 131:3958–3964. [PubMed: 19292490]
12. Hwang S, Kim E, Kwak J. Electrochemical Detection of DNA Hybridization Using Biometallization. Anal. Chem. 2005; 77:579–584. [PubMed: 15649056]
13. Caballero S, Abad FX, Loisy F, Le Guyader FS, Cohen J, Pintó RM, Bosch A. Rotavirus Virus-Like Particles as Surrogates in Environmental Persistence and Inactivation Studies. Appl. Environ. Microbiol. 2004; 70:3904–3909. [PubMed: 15240262]
14. Dahling DR. Detection and enumeration of enteric viruses in cell culture. Critical Reviews in Environmental Control. 1991; 21:237–263.
15. Yeh H-Y, Yates MV, Chen W, Mulchandani A. Real-time molecular methods to detect infective viruses. Sem. Cell Molecul. Dev. Biol. 2009; 20:49–54.
16. Van Emon, JM.; Chuang, JC.; Trejo, RM.; Durnford, J. Integrating bioanalytical capability in an environmental analytical laboratory in Immunoassay and other bioanalytical techniques. Van Emon, JM., editor. Boca Raton: CRC Press; 2007. p. 1-44.
17. Li Z, Chen Y, Li X, Kamins TI, Nauka K, Williams RS. Sequence-Specific Label-Free DNA Sensors Based on Silicon Nanowires. Nano Letters. 2004; 4(2):245–247.
18. Ishikawa FN, Chang HK, Curreli M, Liao H-I, Olson CA, Chen P-C, Zhang R, Roberts RW, Sun R, Cote RJ, Thompson ME, Zhou C. Label-Free, Electrical Detection of the SARS Virus N-Protein with Nanowire Biosensors Utilizing Antibody Mimics as Capture Probes. ACS Nano. 2009; 3(5):1219–1224. [PubMed: 19422193]
19. Huang HM, Mao S, Feick H, Yan H, Wu Y, Kind H, Weber E, Russo R, Yang P. Room-Temperature Ultraviolet Nanowire Nanolasers. Science. 2001; 292:1897–1899. [PubMed: 11397941]
20. Li Y, Qian F, Xiang J, Lieber CM. Nanowire Electronic and Optoelectronic Devices. Mater. Today. 2006; 9:18–27.
21. Patolsky F, Timko BP, Zheng G, Lieber CM. Nanowire-Based Nanoelectronic Devices in the Life Sciences. MRS Bulletin. 2007; 32:142–149.
22. Guo S, Wen D, Dong S, Wang E. Gold Nanowire Assembling Architecture for H_2O_2 Electrochemical Sensor. Talanta. 2009; 77:1510–1517. [PubMed: 19084672]
23. Law M, Greene LE, Johnson JC, Saykally R, Yang P. Nanowire Dye-Sensitized Solar Cells. Nature Materials. 2005; 4:455–459.
24. Sun XW, Wang JX. Fast Switching Electrochromic Display Using a Viologen-Modified ZnO Nanowire Array Electrode. Nano Lett. 2008; 8:1884–1889. [PubMed: 18564881]
25. Elfström N, Karlström AE, Linnros J. Silicon Nanoribbons for Electrical Detection of Biomolecules. Nano Lett. 2008; 8:945–949. [PubMed: 18266330]
26. Martinez JA, Misra N, Wang Y, Stroeve P, Grigoropoulos CP, Noy A. Highly Efficient Biocompatible Single Silicon Nanowire Electrodes with Functional Biological Pore Channels. Nano Lett. 2009; 9:1121–1126. [PubMed: 19203205]
27. Cui Y, Wei Q, Park H, Lieber CM. Nanowire Nanosensors for Highly Sensitive and Selective Detection of Biological and Chemical Species. Science. 2001; 293:1289–1292. [PubMed: 11509722]
28. Hahm J, Lieber CM. Direct Ultrasensitive Electrical Detection of DNA and DNA Sequence Variations Using Nanowire Nanosensors. Nano Lett. 2004; 4:51–54.

29. Patolsky F, Zheng G, Hayden O, Lakadamyali M, Zhuang X, Lieber CM. Electrical Detection of Single Viruses. Proc. Nat. Acad. Sci. 2004; 101:14017–14022. [PubMed: 15365183]
30. Zheng G, Patolsky F, Lieber CM. Multiplexed Electrical Detection of Single Viruses. Mater. Res. Soc. Symp. Proc. 2005; 828 A2.2.
31. Chen RJ, Bangsaruntip S, Drouvalakis KA, Kam NWS, Shim M, Li Y, Kim W, Utz PJ, Dai H. Noncovalent Functionalization of Carbon Nanotubes for Highly Specific Electronic Biosensor. Proc. Nat. Acad. Sci. 2003; 100:4984–4989. [PubMed: 12697899]
32. Angelopoulos M. Conducting polymers in microelectronics. IBM J. Res. Dev. 2001; 45:57–75.
33. Otero, TF. Electrochemomechanical devices based on conducting polymers. In: Osada, Y.; De Rossi, DE., editors. Polymer Sensors and Actuators. Berlin: Springer; 2000. p. 295-324.
34. Bailey, RA.; Persaud, KC. Sensing volatile chemicals using conducting polymer arrays. In: Osada, Y.; De Rossi, DE., editors. Polymer Sensors and Actuators. Berlin: Springer; 2000. p. 149-181.
35. Bangar MA, Shirale DJ, Chen W, Myung NV, Mulchandani A. Single Conducting Polymer Nanowire Chemiresistive Label-Free Immunosensor for Cancer Biomarker. Anal. Chem. 2009; 81:2168–2175. [PubMed: 19281260]
36. Ivanovska I, Wuite G, Jonsson B, Evilevitch A. Internal DNA Pressure Modifies Stability of WT Phage. Proc. Nat. Acad. Sci. 2007; 104:9603–9608. [PubMed: 17535894]
37. Cho M, Chung H, Choi W, Yoon J. Different Inactivation Behaviors of MS-2 Phage and Escherichia coli in TiO2 Photocatalytic Disinfection. Appl. Environ. Microbiol. 2005; 71:270–275. [PubMed: 15640197]
38. Debartolomeis J, Cabelli VJ. Evaluation of an Escherichia Coli Host Strain for Enumeration of F Male-specific Bacteriophages. Appl. Environ. Microbiol. 1991; 57:1301–1305. [PubMed: 1830197]
39. Gupta M, Caniard A, Varela ÁT, Campopiano DJ, Mareque-Rivas JC. Nitrilotriacetic Acid-Derivatized Quantum Dots for Simple Purification and Site-Selective Fluorescent Labeling of Active Proteins in a Single Step. Bioconjugate Chem. 2008; 19:1964–1967.
40. T7 Select System Manual TB178. Madison, WI: Novagen; 2000.
41. Xu Q, Meng G, Han F, Zhao X, Kong M, Zhu X. Controlled Fabrication of Gold and Polypyrrole Nanowires with Straight and Branched Morphologies via Porous Alumina Template-Assisted Approach. Materials Letters. 2009; 63:1431–1434.
42. Hulteen JC, Martin CR. A General Template-based Method for the Preparation of Nanomaterials. J. Mat. Chem. 1997; 7:1075–1087.
43. Joo J, Park KT, Kim BH, Kim MS, Lee SY, Jeong CK, Lee JK, Park DH, Yi WK, Lee SH, Ryu KS. Conducting Polymer Nanotube and Nanowire Synthesized by Using Nanoporous Template: Synthesis, Characteristics, and Applications. Synthetic Metals. 2003; 135–136:7–9.
44. Joo J, Kim BH, Park DH, Kim HS, Seo DS, Shim JH, Lee SJ, Ryu KS, Kim K, Jin J-I, Lee TJ, Lee CJ. Fabrication and Applications of Conducting Polymer Nanotube, Nanowire, Nanohole, and Double Wall Nanotube. Synthetic Metals. 2005; 153:313–316.
45. Kim BH, Park DH, Joo J, Yu SG, Lee SH. Synthesis, characteristics, and field emission of doped and de-doped polypyrrole, polyaniline, poly(3,4- ethylenedioxythiophene) nanotubes and nanowires. Synthetic Metals. 2005; 150:279–284.
46. Joo J, Lee SJ, Park DH, Lee JY, Lee TJ, Seo SH, Lee CJ. Field-Emission Characteristics of Electrochemically Synthesized Polypyrrole Nanotubes Prepared by SDC. Electrochemical and Solid-State Letters. 2005; 8(4):H39–H41.
47. Ackermann J, Videlot C, Nguyen TN, Wang L, Sarro PM, Crawley D, Nikolić K, Forshaw M. Micro-patterning of self-supporting layers with conducting polymer wires for 3D-chip interconnection applications. Appl. Sur. Sci. 2003; 212–213:411–416.
48. Kang DI, Cho WJ, Rhee HW, Ha CS. Electrochemical properties of poly(N-substituted pyrrole)s obtained in TBADS/ACN electrolyte system. Synthetic Metals. 1995; 69:503–504.
49. Park JG, Lee SH, Kim B, Park YW. Electrical resistivity of polypyrrole nanotube measured by conductive scanning probe microscope: The role of contact force. Appl. Phys. Lett. 2002; 81(24): 4625–4627.
50. Janata J, Josowicz M. Conducting polymers in electronic chemical sensors. Nat. Mat. 2003; 2:19–24.

51. Li C, Curreli M, Lin H, Lei B, Ishikawa FN, Datar R, Cote RJ, Thompson ME, Zhou C. Complementary Detection of Prostate-Specific Antigen Using In2O3 Nanowires and Carbon Nanotubes. J. Am. Chem. Soc. 2005; 127:12484–12485. [PubMed: 16144384]

52. Kang DI, Cho WJ, Rhee HW, Ha CS. Electrochemical properties of poly(N-substituted pyrrole)s obtained in TBADS/ACN electrolyte system. Synthetic Metals. 1995; 69:503–504.

53. Reynolds JR, Poropatic PA, Toyooka RL. Electrochemical copolymerization of pyrrole with N-substituted pyrroles. Effect of composition on electrical conductivity. Macromolecules. 1987; 20:958–961.

54. Wick, CH.; Anderson, DM.; McCubbin, PE. Characterization of the Integrated Virus Detection System (IVDS) Using MS2 Bacteriophage. Aberdeen Proving Ground, MD: Edgewood Chemical Biological Center : U.S. Soldier and Bio-logical Chemical Command; 1999. Technical Report ECBC-TR-018

55. Cole KD, Pease LF III, Tsai D-H, Singh T, Lute S, Brorson KA, Wang L. Particle concentration measurement of virus samples using electrospray differential mobility analysis and quantitative amino acid analysis. J. Chromatogr. A. 2009; 1216:5715–5722. [PubMed: 19545873]

56. Zhu H, White IM, Suter JD, Zourob M, Fan X. Opto-fluidic micro-ring resonator for sensitive lebel-free viral detection. Analyst. 2008; 133:356–360. [PubMed: 18299750]

57. Uttenthaler E, Schraml M, Mandel J, Drost S. Ultrasensitive quartz crystal microbalance sensor for detection of M 13-phages in liquids. Biosens. Bioelectron. 2001; 16:735–743. [PubMed: 11679251]

58. Amano Y, Cheng Q. Detection of influenza virus: traditional approaches and development of biosensors. Anal. Bioanal. Chem. 2005; 381:156–164. [PubMed: 15592819]

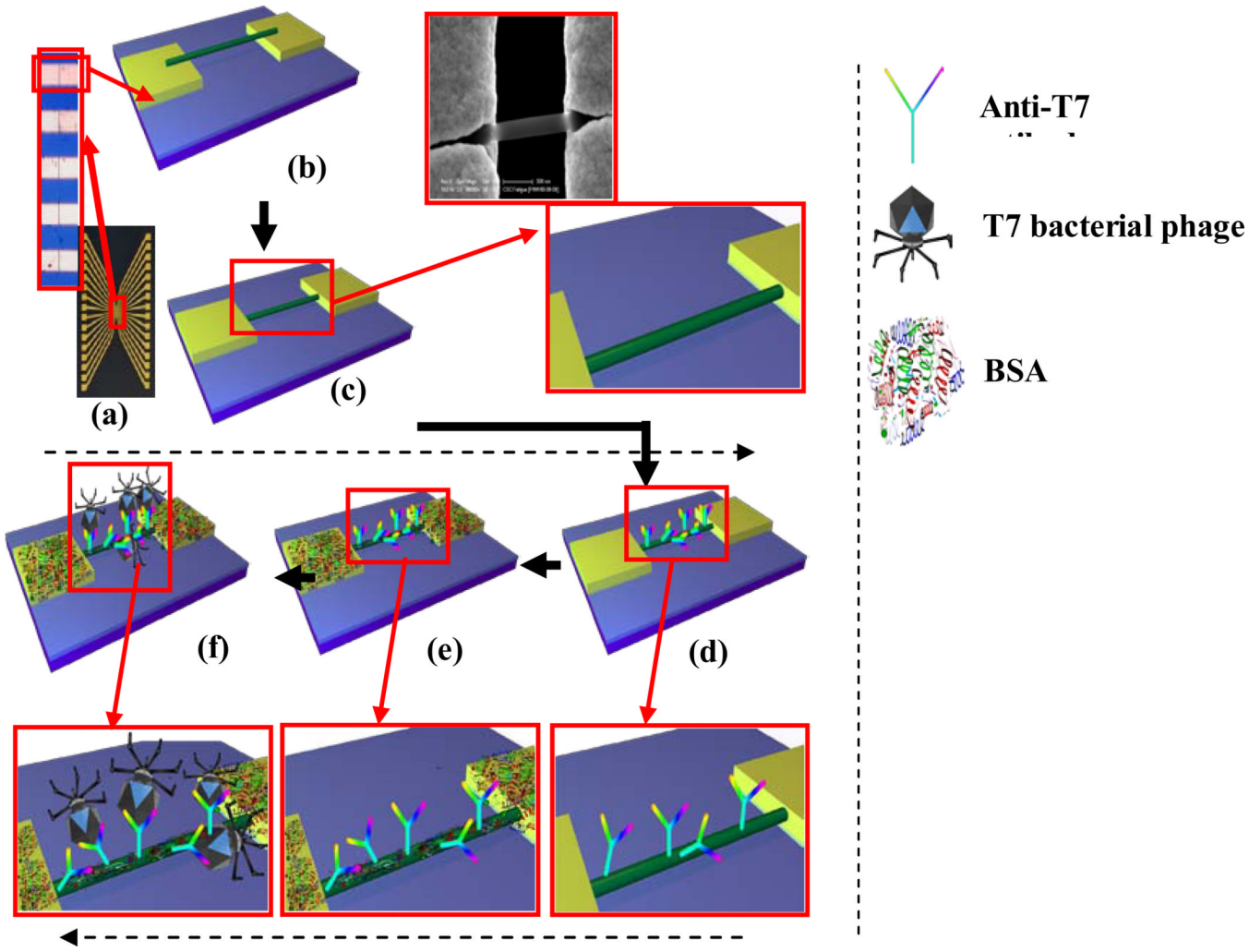

Figure 1.

a) Photo image of 16 electrodes chip (inset optical image showing gap between two electrodes). Schematic of b) aligned and c) anchored Ppy nanowire on the gold electrodes with 3 μm gap (inset: blown up schematic & SEM image). Schematics with blown ups of d) anti-T7 functionalized Ppy nanowire. e) BSA blocking after antibody-functionalization f) T7 phage interacts with anti-T7 antibody on the nanowire surface.

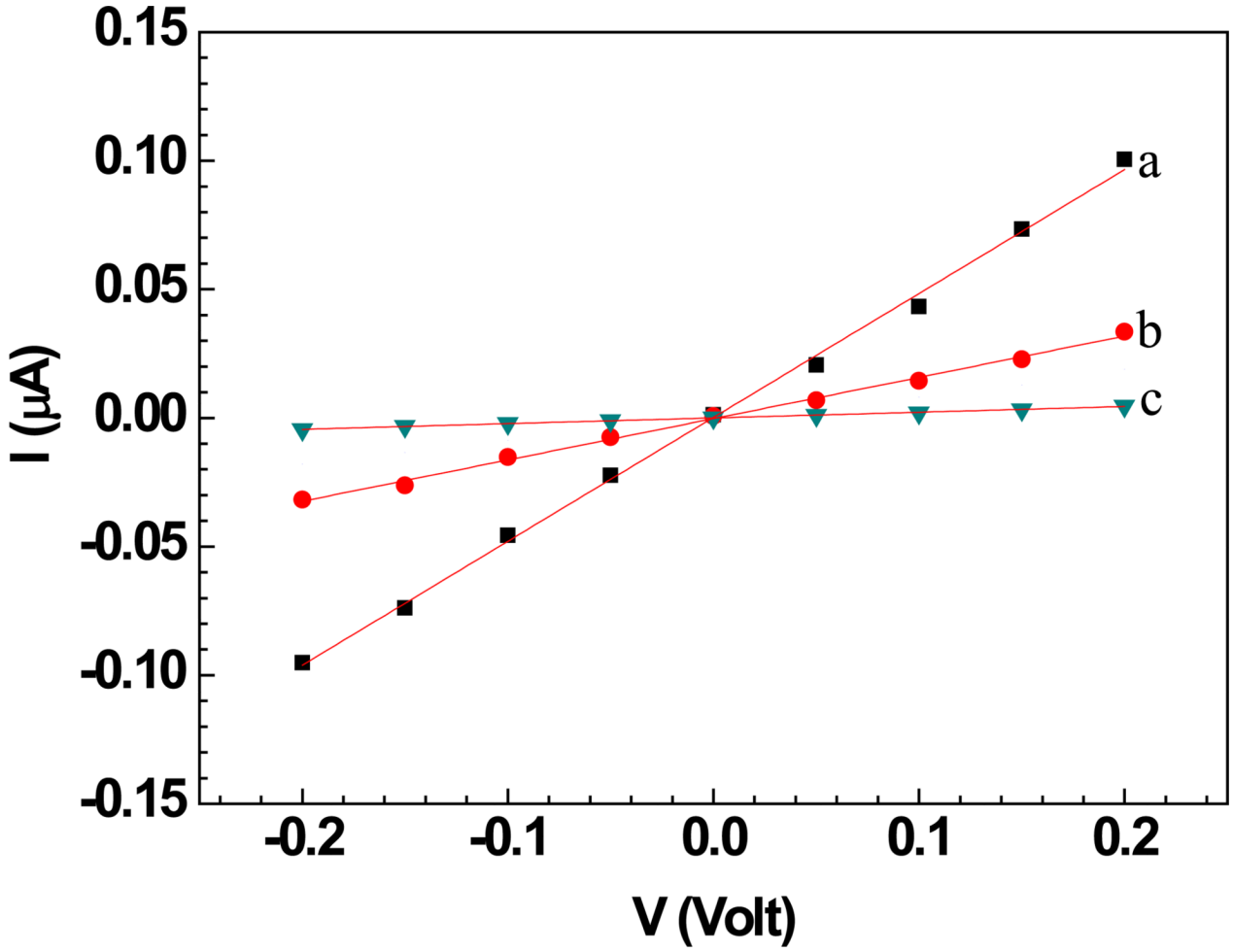

2A

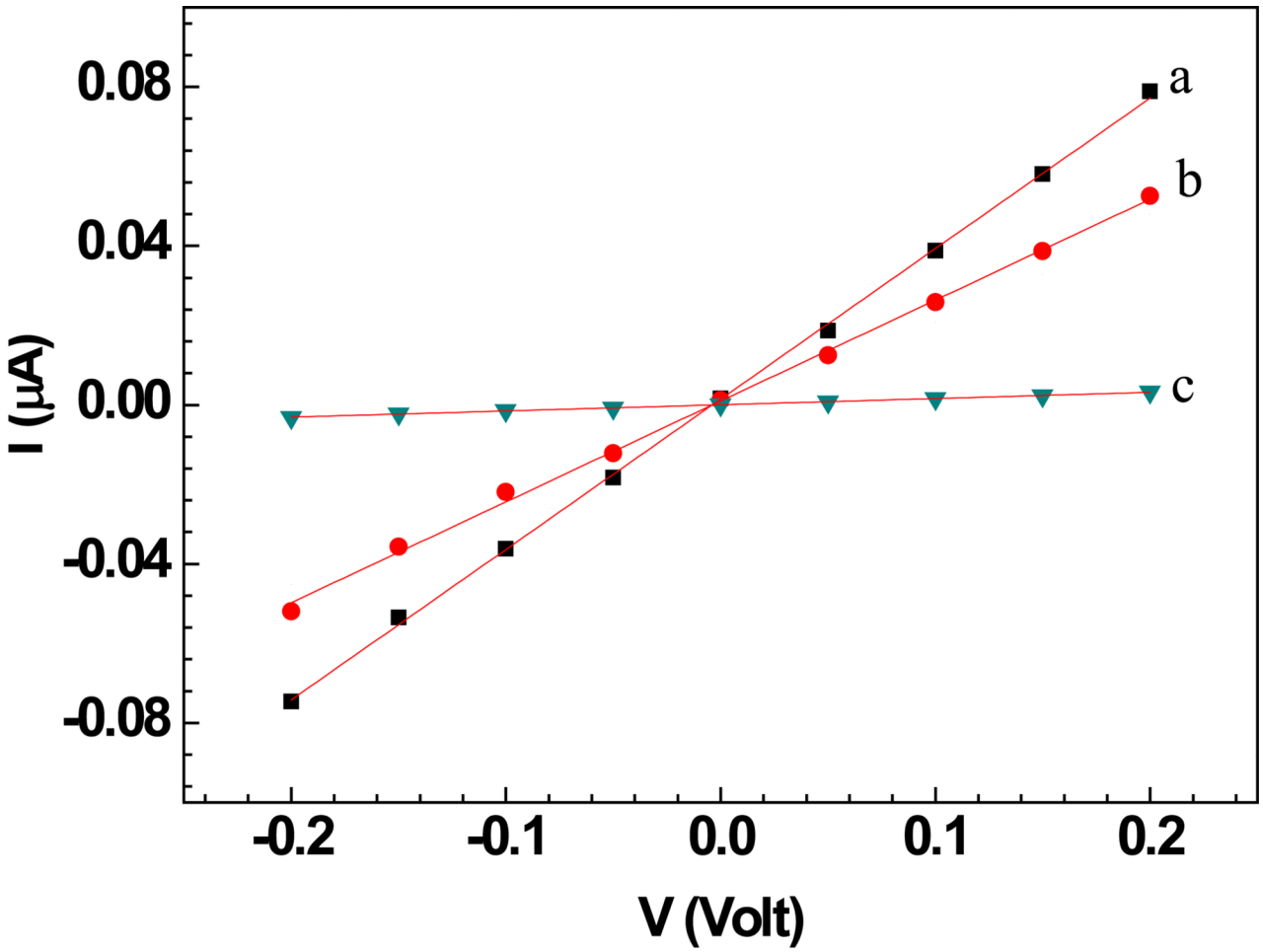

2B

Figure 2.

A: Wet I–V characteristic curves of a a) bare Ppy nanowire b) after anti T7 immobilization and BSA blocking and c) after subsequent incubation with T7 phage (10^9 PFU). Solid lines represent the linear fit.

B: Wet I–V characteristic curves of a a) bare Ppy nanowire b) after anti MS2 immobilization and BSA blocking and c) after subsequent incubation with MS2 phage (10^9 PFU). Solid lines represent the linear fit.

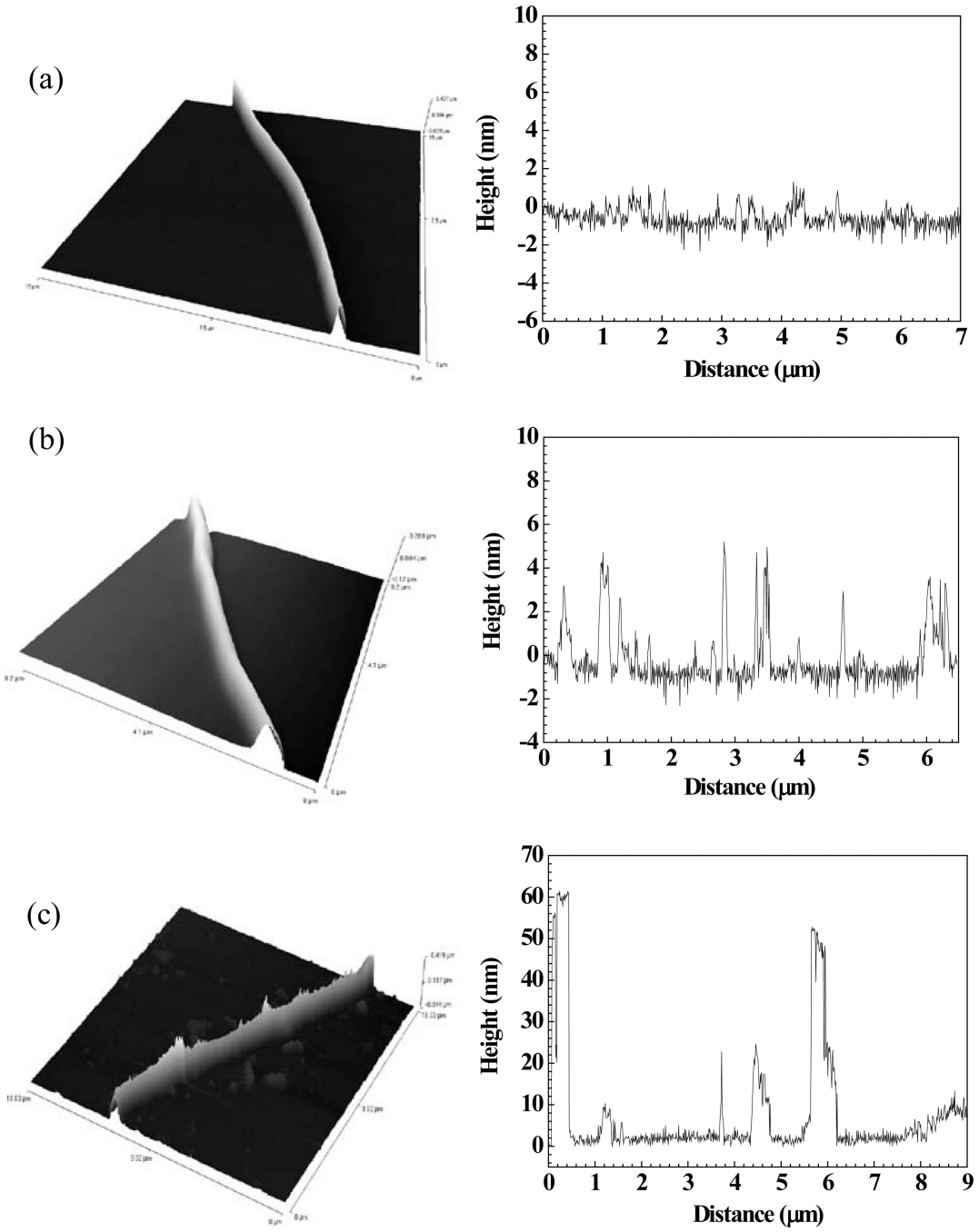

Figure 3.
AFM image and height profile measured along the length of (a) a bare single Ppy nanowire, (b) Ppy nanowire functionalized with anti-T7 antibody and blocked with BSA, and (c) anti-T7 functionalized and BSA blocked Ppy nanowire after T7 bacteriophage binding.

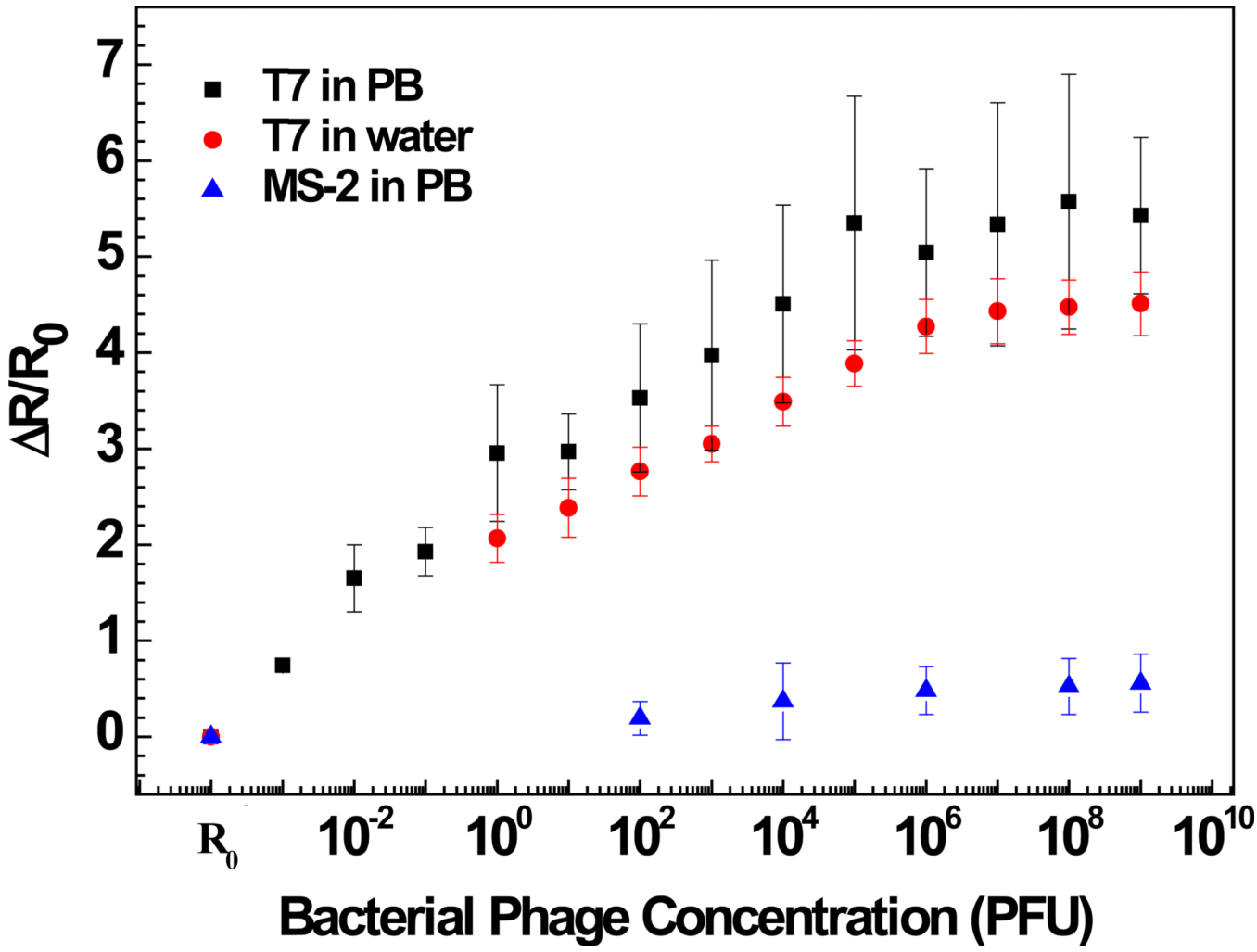

Figure 4.
Sensing response of anti-T7 immobilized Ppy nanowire towards various concentrations of bacteriophages in PB and lake water samples.

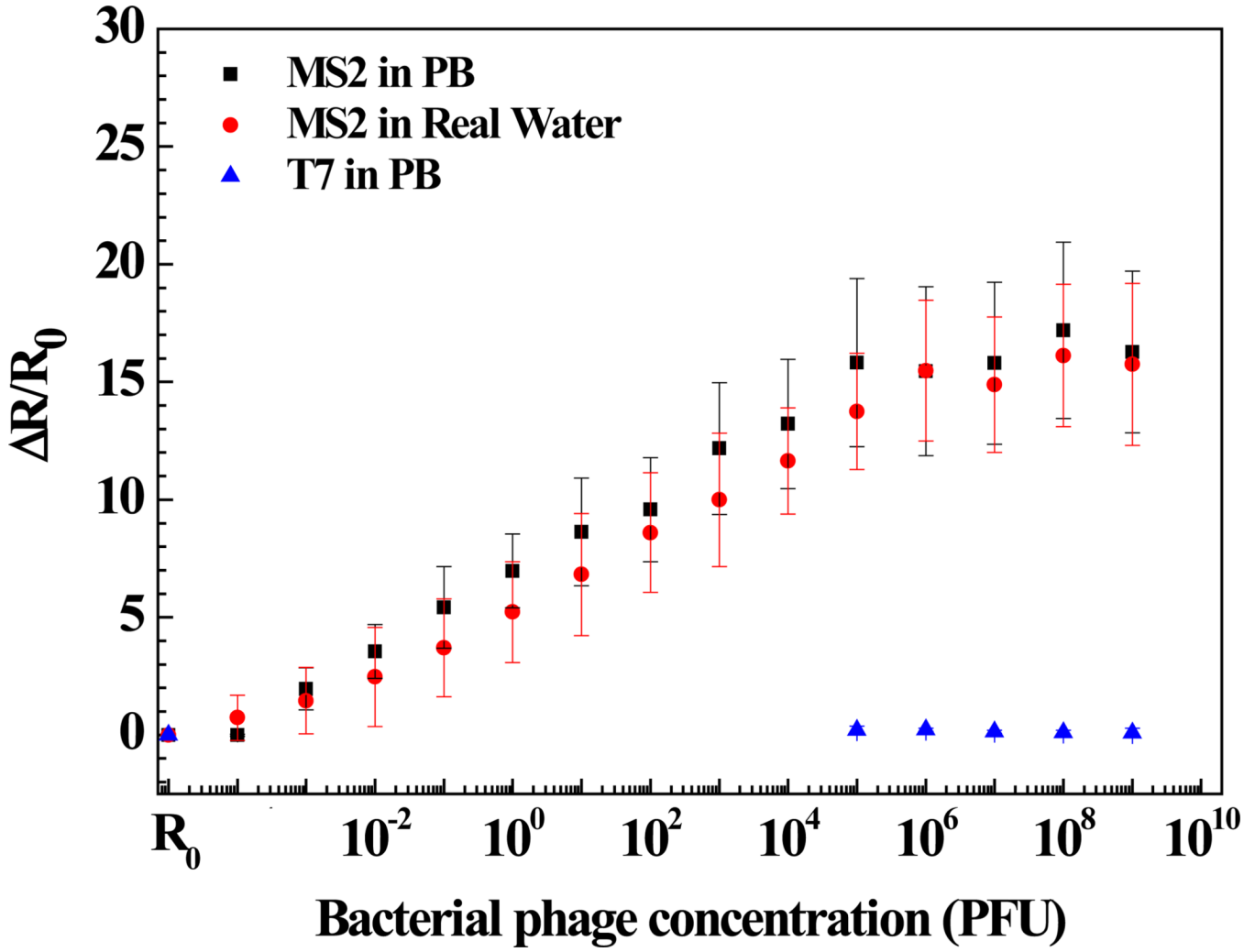

Figure 5.
Sensing response of anti-MS2 immobilized Ppy nanowire towards various concentrations of bacteriophages in PB and lake water samples.